

## Magnetic ordering induced ferroelectricity in $\alpha$ - $\text{Cu}_2\text{V}_2\text{O}_7$ studied through non-magnetic Zn doping

Bidisa Chattopadhyay, Md. A. Ahmed, S. Bandyopadhyay, R. Singha, and P. Mandal

Citation: *Journal of Applied Physics* **121**, 094103 (2017); doi: 10.1063/1.4977859

View online: <http://dx.doi.org/10.1063/1.4977859>

View Table of Contents: <http://aip.scitation.org/toc/jap/121/9>

Published by the *American Institute of Physics*

---

### Articles you may be interested in

[Molecular beam epitaxy of 2D-layered gallium selenide on GaN substrates](#)  
*Journal of Applied Physics* **121**, 094302094302 (2017); 10.1063/1.4977697

[Angular magnetoresistance oscillations in the tunneling conductance of a metallic heterojunction](#)  
*Journal of Applied Physics* **121**, 094307094307 (2017); 10.1063/1.4977870

[Transverse spin relaxation and magnetic correlation in  \$\text{Pr}\_{1-x}\text{Ca}\_x\text{MnO}\_3\$ : Influence of particle size variation and chemical doping](#)  
*Journal of Applied Physics* **121**, 093901093901 (2017); 10.1063/1.4977580

[Thermo-mechanical vibration of a single-layer graphene sheet and a single-walled carbon nanotube on a substrate](#)  
*Journal of Applied Physics* **121**, 094304094304 (2017); 10.1063/1.4977843

---

Applied Physics  
Reviews

SAVE THE DATE!  
**3D Bioprinting: Physical and Chemical Processes**  
May 2–3, 2017 • Winston Salem, NC, USA

## Magnetic ordering induced ferroelectricity in $\alpha$ - $\text{Cu}_2\text{V}_2\text{O}_7$ studied through non-magnetic Zn doping

Bidisa Chattopadhyay,<sup>1,a)</sup> Md. A. Ahmed,<sup>2</sup> S. Bandyopadhyay,<sup>2,3</sup> R. Singha,<sup>4</sup> and P. Mandal<sup>4</sup>

<sup>1</sup>Department of Physics, Lady Brabourne College, P-1/2 Suhrawardy Avenue, Kolkata 700 017, India

<sup>2</sup>Department of Physics, University of Calcutta, 92 A.P.C. Road, Kolkata 700009, India

<sup>3</sup>CRNN, University of Calcutta, JD 2, Sector III, Salt Lake, Kolkata 700098, India

<sup>4</sup>Saha Institute of Nuclear Physics, HBNI, 1/AF Bidhannagar, Kolkata 700 064, India

(Received 21 October 2016; accepted 19 February 2017; published online 7 March 2017)

We have studied the magnetic and electronic properties of  $\text{Cu}_{2-x}\text{Zn}_x\text{V}_2\text{O}_7$  by magnetization, specific heat, and dielectric measurements. X-ray structural analysis shows a Zn-mediated phase transition from the  $\alpha$ - to the  $\beta$ -phase beyond a critical Zn concentration of  $x_c = 0.15$ . While  $\text{Cu}_2\text{V}_2\text{O}_7$  exhibits a canted antiferromagnetism with an associated weak ferromagnetism in the  $\alpha$ -phase, the  $\beta$ -phase is purely antiferromagnetic. The spin canting arises due to the Dzyaloshinskii-Moriya exchange interaction in the anti-symmetric  $\alpha$ -phase. The temperature dependence of the heat capacity for the sample in the  $\alpha$ -phase shows a clear lambda like transition at a temperature where the magnetic susceptibility also displays an anomaly and indicates an onset of long range magnetic ordering. Dielectric properties display a clear anomaly around the magnetic transition temperature in  $\alpha$ - $\text{Cu}_2\text{V}_2\text{O}_7$ . The anomaly weakens with the increase in the Zn concentration and disappears at the doping level where  $\alpha$  to  $\beta$  phase transition occurs. This confirms the existence of magneto-electric coupling in  $\alpha$ - $\text{Cu}_2\text{V}_2\text{O}_7$  but not in its  $\beta$ -phase. Analysis of the experimental data shows that magneto-electric coupling is non-linear in nature, which is in agreement with the Landau theory of continuous phase transition. So,  $\alpha$ - $\text{Cu}_2\text{V}_2\text{O}_7$  establishes itself as a promising candidate for magnetic multiferroics. *Published by AIP Publishing.*

[<http://dx.doi.org/10.1063/1.4977859>]

### I. INTRODUCTION

Multiferroics have attracted a great deal of research interest since the early 2000s due to their wide range of application possibilities as magnetic sensors, multiple state memory devices, spintronics, and so on.<sup>1-3</sup> Although several efforts have been made in searching for new multiferroic materials following different routes, magnetic ordering induced ferroelectricity has become very much interesting and exciting due to their high value of magnetoelectric coupling.<sup>4-7</sup> Ferroelectricity caused by magnetism was first discovered by Kimura *et al.*<sup>8</sup> in the hexagonal manganite  $\text{TbMnO}_3$ . In this material, a non-zero electric polarization appears for a special type of magnetic ordering below 28 K and also a polarization flop occurs when a magnetic field is applied along a certain crystallographic direction. In the same year, in  $\text{TbMn}_2\text{O}_5$ , Hur *et al.*<sup>9</sup> observed an even stronger effect of the external magnetic field on electric polarization. In these systems, a sign change in the electric polarization with the field is noticed. This induces an oscillation in the electric polarization when the magnetic field alternates between +15 kOe and -15 kOe. Hence, multiferroism in these materials is very much useful to prepare new forms of multifunctional devices. This bears the prospect of controlling the spontaneous magnetization by an applied electric field (without currents). At the same time, the spontaneous

electric polarization can be reoriented by an applied magnetic field. This is attributed to the strong coupling between the two order parameters. Moreover, many open issues are there concerning the basic electronic and magnetic structures in this class of compounds and the cross coupling between their order parameters. An efficient coupling between two order parameters is even more important than their coexistence.

Copper based divanadates ( $\text{Cu}_2\text{V}_2\text{O}_7$ ) generally occur in two polymorphs that are stable, low temperature  $\alpha$  phase and high temperature  $\beta$  phase.<sup>10,11</sup> The phase transition temperature is 712 °C. The structure of the  $\alpha$  phase is orthorhombic and noncentrosymmetric with  $Fdd2$  symmetry, whereas the  $\beta$  phase is monoclinic and centrosymmetric with  $C2/c$  symmetry. The high temperature  $\beta$  phase is isostructural with that of  $\alpha$ - $\text{Zn}_2\text{V}_2\text{O}_7$ . In the  $\alpha$  phase, each  $\text{Cu}^{2+}$  ion is surrounded by five oxygen ions forming a distorted polyhedron, and these polyhedra are attached with one another by edge sharing.<sup>12,13</sup> Such  $\text{CuO}_5$  complexes form two mutually perpendicular spin chains forming a honeycomb like spin structure, which are separated by  $(\text{V}_2\text{O}_7)^{-2}$  anion groups, consisting of a corner sharing  $[\text{VO}_4]$  tetrahedron as shown in Fig. 1. In copper divanadates, magnetic moment arises completely from  $\text{Cu}^{2+}$  cations having  $3d^9$  electronic configuration since  $\text{V}^{5+}$  ( $3d^0$ ) is nonmagnetic. The magnetic structure of the  $\alpha$  phase is reported to be an antiferromagnet with weak ferromagnetism (FM) at low temperatures and the  $\beta$  phase to be a linear chain antiferromagnet with a uniform

<sup>a)</sup>Author to whom correspondence should be addressed. Electronic mail: bidisa\_chattopadhyay@rediffmail.com

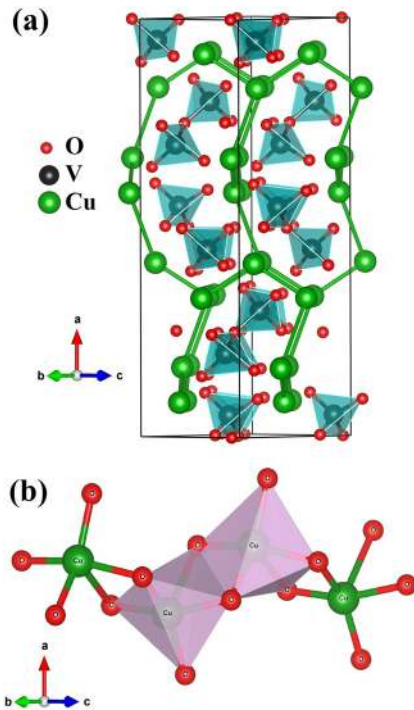


FIG. 1. (a) Crystal structure of  $\alpha$ - $\text{Cu}_2\text{V}_2\text{O}_7$  where Cu atoms form two mutually perpendicular spin chains with  $\text{CuO}_5$  complexes separated by  $(\text{V}_2\text{O}_7)^{2-}$  anion groups. (b) Clear view of edge sharing  $\text{CuO}_5$  polyhedra where each  $\text{Cu}^{2+}$  ion is surrounded by five oxygen ions. The structures are visualized using VESTA.

intrachain interaction.<sup>11–17</sup> The study of the dielectric behaviour of  $\alpha$ - $\text{Cu}_2\text{V}_2\text{O}_7$  around the magnetic transition temperature looking for a possible coupling between their dielectric and magnetic properties has reported  $\alpha$ - $\text{Cu}_2\text{V}_2\text{O}_7$  to be a magnetic multiferroic with the simultaneous development of electric polarization and magnetization below  $T_N = 35$  K.<sup>12,15</sup> From the reported magnetic studies of  $\alpha$ - $\text{Cu}_2\text{V}_2\text{O}_7$ ,<sup>11–17</sup> we know that this system undergoes a transition to a magnetically ordered state below the Neel temperature  $T_N = 35$  K, which is attributed to a canted antiferromagnetic (AF) transition of the Cu spin ( $S = 1/2$ ). This result is a signature of the Dzyaloshinskii-Moriya (DM) interaction between the neighboring Cu spins in the  $\alpha$  phase due to its antisymmetric exchange interaction. On the other hand, the  $\beta$  phase is forbidden by the DM interaction due to its symmetric spin structure, which leads to no associated weak ferromagnetism (FM). Pommer *et al.*<sup>17</sup> showed a Zn mediated phase transition from the  $\alpha$  phase to the  $\beta$  phase by nonmagnetic Zn doping at the Cu site in the  $\alpha$ - $\text{Cu}_2\text{V}_2\text{O}_7$  system beyond a critical Zn concentration  $x_c = 0.15$ . Moreover, the static magnetic properties change drastically, and no clear evidence of weak ferromagnetism is identified in the  $\beta$  phase when the Zn concentration exceeds the critical value.<sup>18</sup> Very few dielectric studies have been made so far for this compound, which have reported the presence of dielectric anomaly around the Neel temperature ( $T_N$ ) in the  $\alpha$  phase only.<sup>12,15</sup> Recently, based on density functional theory calculations and magneto-dielectric studies, Sannigrahi *et al.*<sup>12</sup> proposed an exchange striction based mechanism for the giant ferroelectric polarization ( $\sim 0.55 \mu\text{Ccm}^{-2}$ , highest among the copper based improper

multiferroics) observed in polycrystalline  $\alpha$ - $\text{Cu}_2\text{V}_2\text{O}_7$ , which generally occurs in collinear magnetic structures. On the other hand, Gitgeatpong *et al.*<sup>13</sup> proposed a helical-honeycomb model leading to the DM interaction<sup>19,20</sup> to describe the magnetic ordering observed in a single crystal of  $\alpha$ - $\text{Cu}_2\text{V}_2\text{O}_7$  based on combined studies of magnetization, Quantum Monte Carlo simulations, and neutron diffraction. Recently, a third mechanism was also proposed by Lee *et al.*<sup>21</sup> based on structural, magnetic, and dielectric studies on the same material in single crystalline and polycrystalline forms. They proposed a p-d hybridization scheme due to spin orbit coupling which is of purely electronic origin in contrast to the ion-displacement type occurring in the spin-current mechanism or exchange striction based mechanism reported so far. So, it is clear that the underlying mechanism for the magneto-electric coupling in this material is still in debate.

In this work, we have reported the phase evolution of the copper divanadate system from the  $\alpha$ - to the  $\beta$ -phase through nonmagnetic Zn substitution at the Cu site and the results of the magnetic and electronic properties measurement covering the Zn-doping range  $0 \leq x \leq 0.3$ . The magnetic properties have been discussed in the light of the DM interaction present only in the non-collinear magnetic structure. The results of the temperature dependence of zero-field heat capacity measurement and the dielectric properties' measurement have been presented to confirm the existence of magnetic ordering induced ferroelectricity in  $\alpha$ - $\text{Cu}_2\text{V}_2\text{O}_7$  with a non-collinear magnetic structure but not in its  $\beta$ -phase having a collinear magnetic structure. The nature of the magneto-electric coupling in this material has also been discussed performing an analysis of the magnetization and dielectric data.

## II. EXPERIMENTAL

Polycrystalline samples of  $\text{Cu}_{2-x}\text{Zn}_x\text{V}_2\text{O}_7$  with  $x = 0-0.3$  were prepared following the standard solid-state reaction technique. Stoichiometric amounts of CuO, ZnO, and  $\text{V}_2\text{O}_5$  were mixed homogeneously using ethanol. The mixture was then annealed in air at  $600^\circ\text{C}-650^\circ\text{C}$  for 100 h–130 h with intermediate grindings. Finally, the powder was pressed into pellets using polyvinyl alcohol as a binder and sintered at  $600^\circ\text{C}-650^\circ\text{C}$  for 10 h. X-ray powder diffraction was used to characterize the samples using a Rigaku TTRAX II diffractometer with Cu-K $\alpha$  radiation in the  $2\theta$  range  $10^\circ-80^\circ$ . Magnetic measurements were done under a field of 5 kOe to 20 kOe in the temperature range  $2\text{ K} \leq T(\text{K}) \leq 300\text{ K}$  using a Quantum Design Superconducting Quantum Interference Device (SQUID) magnetometer. The zero-field heat capacity measurement was carried out in a physical properties' measurement system (Quantum Design). The dielectric measurements were carried out in a two-probe setup with conducting silver paste and gold wire, using a Cryogenic Instrument cryostat operating over a temperature range 2–300 K. An Andeen Hagerling ultra precision capacitance bridge (Model AH2700A) was used in the frequency range 1–20 kHz.

## III. RESULTS AND DISCUSSION

In Fig. 2, we have plotted the x-ray diffraction data for  $\text{Cu}_{2-x}\text{Zn}_x\text{V}_2\text{O}_7$  having different Zn concentrations together



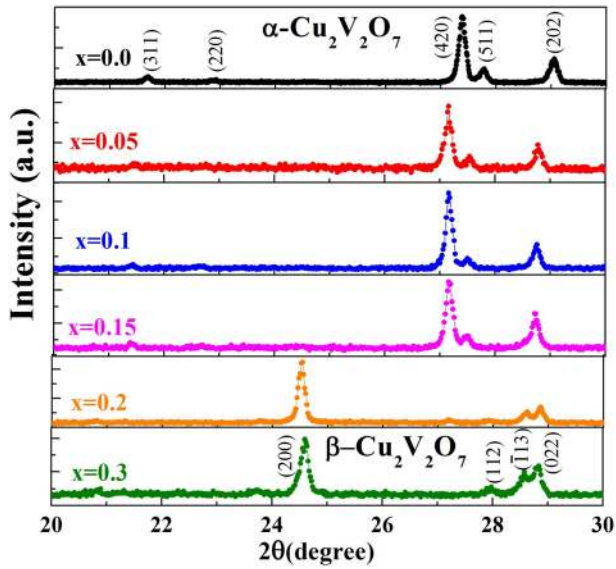


FIG. 2. XRD patterns for  $\text{Cu}_{2-x}\text{Zn}_x\text{V}_2\text{O}_7$  for  $2\theta$  in the range  $20^\circ$  to  $30^\circ$ .

with undoped  $\text{Cu}_2\text{V}_2\text{O}_7$ . For clarity, the curves were shifted vertically. Rietveld analysis shows that the samples are of single phase with  $Fdd2$  symmetry having an orthorhombic crystal structure up to  $x = 0.15$ . A Zn mediated phase transition from the  $\alpha\text{-Cu}_2\text{V}_2\text{O}_7$  to the  $\beta\text{-Cu}_2\text{V}_2\text{O}_7$  phase is clearly observed beyond the critical Zn concentration  $x_c = 0.15$ , in agreement with Pommer *et al.*<sup>17</sup> and Sotojima *et al.*<sup>18</sup>  $\beta\text{-Cu}_2\text{V}_2\text{O}_7$  crystallizes in a monoclinic ( $C2/c$ ) structure. The variation of lattice parameters for different Zn concentrations as obtained by Rietveld studies for  $\alpha\text{-Cu}_2\text{V}_2\text{O}_7$  is summarized in Table I, which are consistent with the existing literature.<sup>15,18</sup>

In Fig. 3, the zero field cooled magnetic susceptibility is plotted as a function of temperature for the Zn-doped samples (up to  $x_c = 0.15$ ) along with the undoped one in a magnetic field  $H = 0.5$  kOe. As the temperature lowers,  $\chi(T)$  shows a steep upturn around  $T_N$ , indicating a transition to a magnetically ordered state. This behaviour continues up to Zn concentration  $x_c = 0.15$ . We have fitted the inverse of the susceptibility ( $\chi^{-1}$ ) as a function of temperature ( $T$ ) above 80 K using the Curie-Weiss law ( $\chi = \frac{C}{T-\theta}$ ). A representative plot for a Curie-Weiss law fit for  $x = 0.1$  is shown in the inset of Fig. 3. The negative Curie-Weiss temperature ( $\theta$ ) for all the samples (Table I) indicates that the dominant exchange interaction is AF in nature. From the Curie-Weiss constant  $C$ , we have calculated the effective magnetic moment ( $\mu_{eff}$

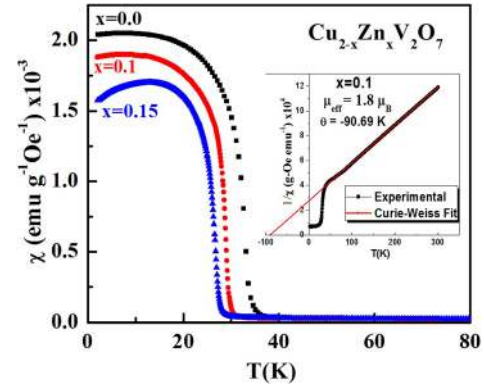


FIG. 3. Zero-field-cooled magnetic susceptibility ( $\chi$ ) as a function of temperature of  $\text{Cu}_{2-x}\text{Zn}_x\text{V}_2\text{O}_7$  measured at 500 Oe. The inset shows the inverse of susceptibility ( $\chi^{-1}$ ) for  $x = 0.1$  and the corresponding Curie-Weiss fit (Solid line).

$= \sqrt{\frac{3k_B C}{N_A}}$ ). It is found to be  $2.09 \mu_B$  for the undoped sample, which is slightly greater than the spin only value  $\mu_{eff} = g\mu_B \sqrt{S(S+1)} = 1.73\mu_B$ , where  $g = 2$  and  $s = \frac{1}{2}$  per  $\text{Cu}^{2+}$  ion consistent with the earlier reports.<sup>12,13,17,18</sup> This may be due to some amount of mixing of the orbital moment, which is a characteristic of the  $\text{Cu}^{2+}$  cation.  $T_N$  (32.8 K for  $x = 0.0$  to 21.4 K for  $x = 0.3$ ) and  $\mu_{eff}$  ( $2.09 \mu_B$  for  $x = 0.0$  to  $1.7 \mu_B$  for  $x = 0.15$ ) gradually decrease with the Zn concentration, which is expected since nonmagnetic Zn dilutes the local spin arrangement within the lattice. The magnitude of  $\theta$  decreases in the  $\alpha$ -phase showing a sudden increase around the phase transition point and thereby maintains its decreasing behaviour up to the highest Zn doping level, in agreement with Pommer *et al.*<sup>17</sup> It is predicted that as Zn doping increases, the nearest neighbour Cu-Cu magnetic exchange interaction gets disturbed since nonmagnetic Zn substitutes magnetic Cu atoms, and as a result, the effective average magnetic exchange interaction may decrease. This may be taken as dilution of effective spin density via Zn doping. As the Zn concentration increases beyond  $x_c = 0.15$ , static magnetic properties change drastically. Instead of showing a steep upturn as the temperature lowers,  $\chi$  first shows a broad maximum at a temperature  $T_{max}$  (39 K and 36 K for  $x = 0.2$  and 0.3, respectively) slightly greater than  $T_N$ , indicating an appearance of a short range correlation typical for a low dimensional magnet (Fig. 4). After that, a sudden increase in  $\chi$  is shown by the  $x = 0.2$  sample around 25.5 K, indicating an onset of weak magnetic ordering at lower temperature. However, a small cusp is observed around  $T_N = 21.4$  K for the  $x = 0.3$  sample as shown in Fig. 4, which is due to the transition to a pure AF state. The broad maximum around  $T_{max}$  slightly greater than  $T_N$  for the samples  $x = 0.2$  and 0.3 is a signature of a one dimensional Heisenberg antiferromagnet. We know that, in  $\text{Cu}_2\text{V}_2\text{O}_7$ ,  $\text{CuO}_5$  complexes form two mutually perpendicular spin chains. To further explore the nature of the magnetic ordering in this region, we have calculated the intrachain nearest-neighbour exchange constant  $J$ , i.e., magnetic exchange between nearest-neighbour Cu-Cu spins along a spin chain from the relation  $T_{max} = \frac{0.641J}{k_B}$ .<sup>17</sup> For the  $x = 0.3$  sample,  $J$  is found to be  $\sim 56$  K. The strength of

TABLE I. Different characterizing parameters for  $\alpha\text{-Cu}_{2-x}\text{Zn}_x\text{V}_2\text{O}_7$  (orthorhombic,  $Fdd2$  symmetry).

Parameters	X=0.0	X=0.05	X=0.1	X=0.15
$a$ (Å)	20.6627	20.6639	20.6642	20.6710
$b$ (Å)	8.4025	8.3926	8.3811	8.3701
$c$ (Å)	6.4419	6.4467	6.4505	6.4548
$V$ (Å <sup>3</sup> )	1118.4314	1117.9993	1117.1514	1116.8060
$T_N$ (K)	32.8	31.6	28.9	26.65
$\theta$ (K)	-82.9	-75.97	-89.38	-50.69
$C_{max}$ (T) (J/mole-K)	...	...	...	31.135

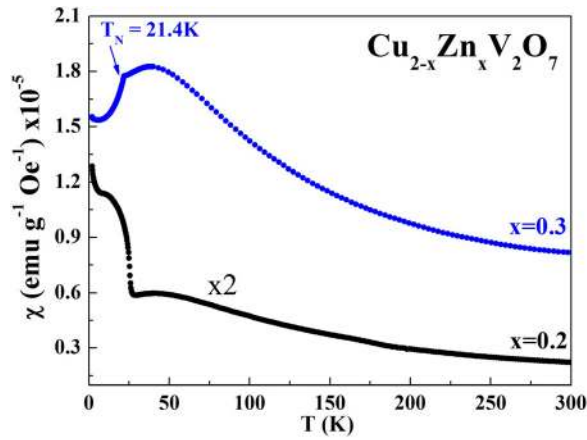


FIG. 4. Zero-field-cooled magnetic susceptibility ( $\chi$ ) as a function of temperature of  $\text{Cu}_{2-x}\text{Zn}_x\text{V}_2\text{O}_7$  measured at 500 Oe for  $x=0.2$  and  $0.3$ . For clarity,  $\chi(T)$  for  $x=0.2$  is magnified 2 times.

the interchain coupling  $J_{\text{inter}}$  can also be estimated from the relation  $J_{\text{inter}} = \frac{T_N}{1.28 \sqrt{\ln(\frac{5.8J}{T_N})}}$  in the mean-field approximation.<sup>17</sup> Using  $J = 56$  K and  $T_N = 21.4$  K,  $J_{\text{inter}}$  is found to be  $\sim 10$  K, only 5.6 times smaller than intrachain interaction  $J$ . Moreover,  $T_{\text{max}}$  is only 1.7 times as large as  $T_N$ . So, it may be suggested that existence of such a significant interchain coupling  $J_{\text{inter}}$  along with intrachain interaction  $J$  drives the system into a magnetically ordered state. All these results together with the nature of variation of  $\theta$  with the Zn concentration may indicate the presence of a three dimensional cooperative ordering of the Cu chains in the system at low temperatures.

The field dependence of magnetization  $M(H)$  measured at temperature 2 K (below Neel temperature  $T_N$ ) up to a maximum field of 20 kOe shows clear hysteresis for all the samples up to Zn concentration  $x_c = 0.15$  as shown in Fig. 5. But the magnetization measured at temperature 50 K (above  $T_N$ ) shows no hysteresis rather a linear behaviour throughout the measured field range. The hysteresis loop, which is a characteristic for FM along with no indication of magnetization saturation up to the highest measured magnetic field, indicates

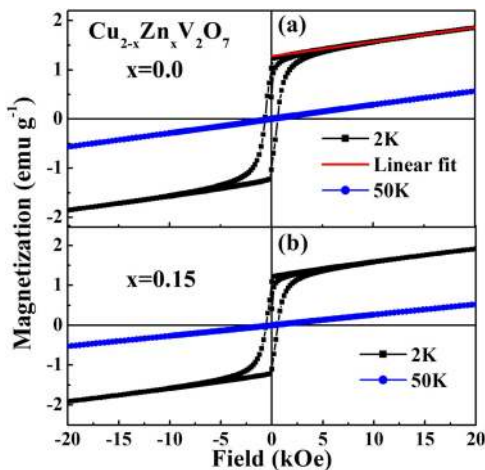


FIG. 5. Field dependence of magnetization data of  $\text{Cu}_{2-x}\text{Zn}_x\text{V}_2\text{O}_7$  for  $x=0.0$  and  $x=0.15$  at 2 K and 50 K along with the linear fitting of the high field data for  $x=0.0$  in (a).

the presence of a canted AF Cu spin arrangement in the material with an associated weak ferromagnetism. Such a canted AF is a signature of the DM interaction between the neighboring Cu spins in the  $\alpha$ -phase of  $\text{Cu}_2\text{V}_2\text{O}_7$  due to the lack of inversion centre between magnetic  $\text{Cu}^{2+}$  ions.<sup>13</sup> On the other hand, the  $x=0.2$  sample shows a very small hysteresis up to  $H=2000$  Oe below  $T_N$  (as shown in the inset of the magnified low field part of Fig. 6) followed by a linear  $M(H)$  behaviour up to the highest applied magnetic field (Fig. 6). This result may be attributed to the sudden increase in  $\chi(T)$  for the  $x=0.2$  sample around 25.5 K (Fig. 4), indicating an onset of weak magnetic ordering at lower temperature with a small residue of magnetization. But a distinctly clear linear  $M(H)$  curve throughout the measured magnetic field range both below and above  $T_N$  without any trace of hysteresis is shown by the  $x=0.3$  sample, which indicates its pure AF behaviour (as shown in the inset of Fig. 6).

We have fitted our high field linear  $M(H)$  data to the empirical relation  $M(H) = \chi_{\text{AF}}H + M(0)$  (as shown in Fig. 5) where the linear term gives the AF component and the second term  $M(0)$  denotes the saturation magnetization, i.e., the canted moment at zero field.  $M(0)$  is found to be  $0.038 \mu_B/\text{Cu-ion}$  for the undoped sample, consistent with other reported values.<sup>12,13,17,22</sup> Such a small value of  $M(0)$  compared to one  $\mu_B$  for the full saturation moment of a single  $\text{Cu}^{2+}$  ion justifies the presence of a canted AF with an associated weak FM in this material. Moreover, the value of  $M(0)$  remains invariant up to  $x_c = 0.15$ , in agreement with Pommer *et al.*<sup>17</sup> So, saturation magnetization that may be a measure of the canting angle through the relation  $\tan \varphi_{\text{DM}} = \frac{M(0)}{g\mu_B S}$  is found to be  $\sim 2^\circ$ , which is the same for all Zn doped samples up to  $x_c = 0.15$ .<sup>17,20</sup> This indicates that in the  $\alpha$ -phase, Zn doping does not change the nature of the exchange interaction but may weaken the strength of the average AF exchange interaction between neighbouring Cu-spins, and as a result,  $T_N$  decreases. Although we have got slight hysteresis in the very low magnetic field region for  $x=0.2$ , the  $M(0)$  for this sample approaches zero as expected (see Fig. 6). So, from our magnetic studies, we may conclude that canted AF Cu spin arrangement due to the DM

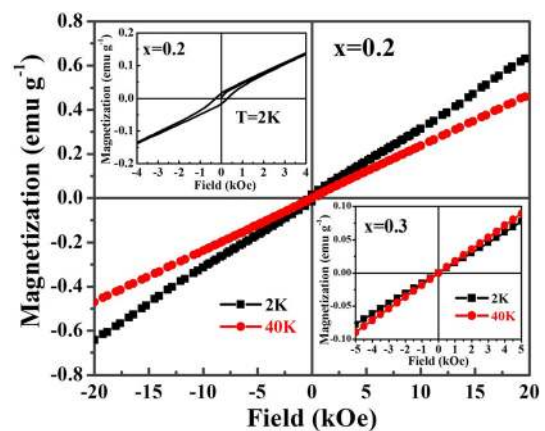


FIG. 6. Field dependence of magnetization data of  $\text{Cu}_{2-x}\text{Zn}_x\text{V}_2\text{O}_7$  for  $x=0.2$  at 2 K and 40 K. The left inset shows the magnified low field part of 2 K for  $x=0.2$ . The right inset shows the field dependence of magnetization data for  $x=0.3$  at 2 K and 40 K.

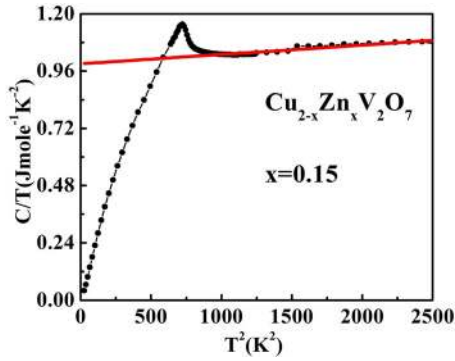


FIG. 7. Temperature dependence of the heat capacity of  $\text{Cu}_{2-x}\text{Zn}_x\text{V}_2\text{O}_7$  for the  $x=0.15$  sample at the zero magnetic field plotted as  $C/T$  versus  $T^2$ . The dashed line gives the best fit in the temperature range 30 K to 50 K above  $T_N$  to  $C(T) = \gamma T + \beta T^3$ .

interaction with an associated weak ferromagnetism exists only in the  $\alpha$ -phase of  $\text{Cu}_{2-x}\text{Zn}_x\text{V}_2\text{O}_7$ .

The temperature dependence of the heat capacity ( $C$ ) of  $\text{Cu}_{2-x}\text{Zn}_x\text{V}_2\text{O}_7$  for the  $x_c=0.15$  sample at zero magnetic field plotted in  $C/T$  versus  $T^2$  coordinates is shown in Fig. 7. A clear lambda-like anomaly observed around Neel temperature  $T_N \sim 26.65$  K reaffirms the existence of a magnetic phase transition in this system. A maximum value of heat capacity  $C_{\text{max}}$  around Neel temperature  $T_N$  is found to be 31.135 J/mole-K (Table I). We have fitted our heat capacity data in the intermediate temperature range 30 K to 50 K above  $T_N$  to  $C(T) = \gamma T + \beta T^3$  as shown in Fig. 7. The best fit result gives  $\gamma = 0.99018 \text{ J mole}^{-1} \text{ K}^{-2}$  and  $\beta = 3.92838 \times 10^{-5} \text{ J mole}^{-1} \text{ K}^{-4}$ , which differs slightly from those for multiferroic  $\text{FeVO}_4$  samples obtained for the same high temperature range.<sup>23,24</sup> From the  $\beta$  value, the Debye temperature has been estimated to be  $\sim 816$  K, which is in good agreement with the reported values of other multiferroic materials.<sup>23,24</sup>

In Fig. 8, we have summarized the temperature variation of the real part of the complex dielectric susceptibility ( $\epsilon'$ ) for  $\text{Cu}_{2-x}\text{Zn}_x\text{V}_2\text{O}_7$  with varying Zn concentrations for a frequency range 1 kHz to 20 kHz. It is found that at low temperature,  $\epsilon'$  shows no temperature and frequency dependence. In the high temperature side,  $\epsilon'$  shows frequency dispersion with a decreasing behavior as the frequency increases. This happens for undoped and for every Zn doped sample. This behavior is consistent with frequency dependence of the static dielectric constant of a dielectric material. But by observing distinctly the low temperature region around  $T_N$ , a clear hump-like anomaly is found for the undoped ( $x=0.0$ ) sample, which gradually loses its prominence but exists up to the critical Zn concentration  $x_c=0.15$ , announcing a transition to a ferroelectric state similar to that observed in other multiferroics.<sup>25</sup> No frequency dispersion is observed for this hump-like anomaly, indicating the appearance of a long range electric order. To analyze the anomaly around  $T_N$ , following Fox *et al.*<sup>26</sup> for  $\text{BaMnF}_4$  and Sánchez-Andújar *et al.*<sup>15</sup> for  $\text{M}_2\text{V}_2\text{O}_7$  ( $M = \text{Co}$  and  $\text{Cu}$ ), we have fitted our dielectric data with the expression (1) to include the lattice contribution of the dielectric constant

$$\epsilon'(T) = \epsilon'(0) + C_0 \left/ \left[ \exp\left(\frac{\hbar\omega_0}{K_B T}\right) - 1 \right] \right. \quad (1)$$

$T_N$  anomalies are clearly envisaged if we plot the variation of  $\epsilon'$  vs.  $T$  along with the fitted curve. A representative plot for  $x=0.0$  is shown in Fig. 9. Sánchez-Andújar *et al.*<sup>15</sup> tried to explain this coupling between dielectric properties and magnetization with the help of the Landau theory of continuous phase transition, which predicts a non-linear magneto-electric coupling,  $\Delta\epsilon' \propto M^2$  (where  $M = \text{magnetization}$ ). Here,  $\Delta\epsilon'$  is defined as the difference between the observed dielectric constant and the lattice contribution. The proportionality between

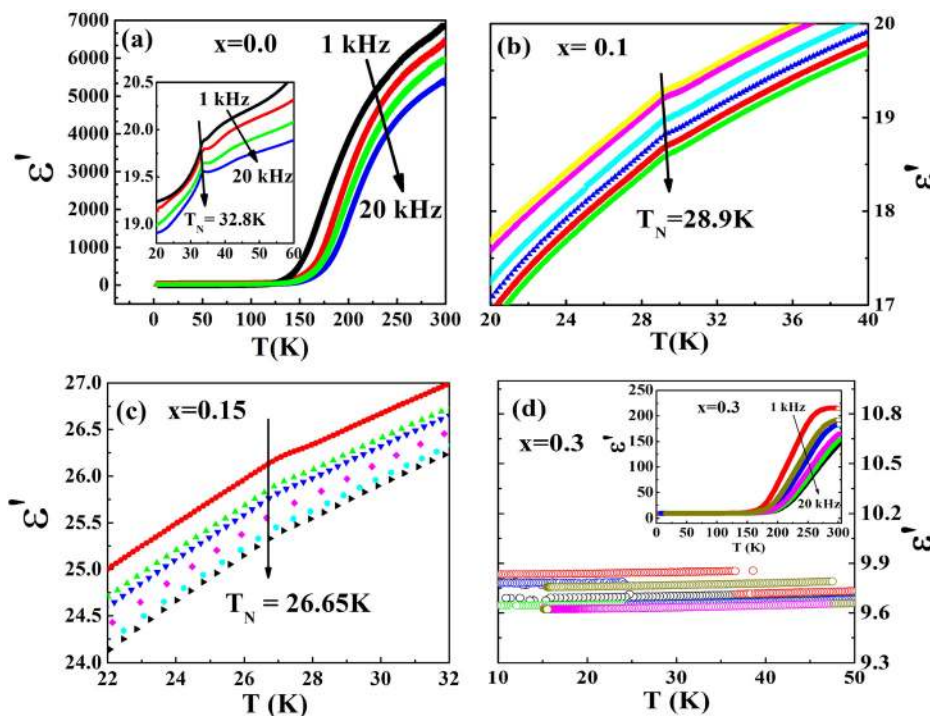


FIG. 8. (a) Temperature dependence of the real part of the dielectric susceptibility ( $\epsilon'$ ) for  $x=0.0$  for the frequency range 1 kHz–20 kHz. The inset shows the magnified low frequency part. (b) and (c) The magnified low frequency part, indicating clearly the presence of hump like anomaly for  $x=0.1$  and  $0.15$ . (d) and its inset confirm the absence of  $\epsilon'$  anomaly for  $x=0.3$ .



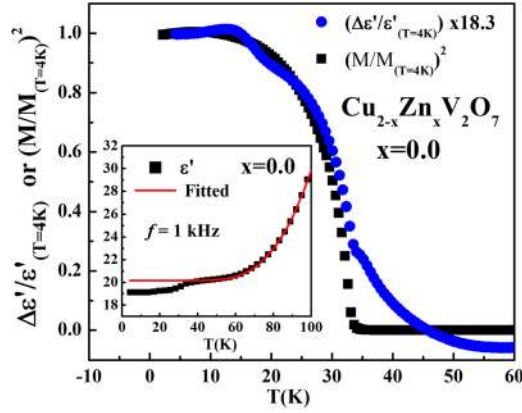


FIG. 9. Plot between normalized  $\Delta\epsilon'$  (difference between the observed dielectric constant and its lattice contribution) and normalized  $M^2$ , indicating the non-linear magneto-dielectric coupling in  $\alpha$ - $\text{Cu}_2\text{V}_2\text{O}_7$ . The inset shows dielectric anomaly in  $\alpha$ - $\text{Cu}_2\text{V}_2\text{O}_7$ , and the curve is a fit to Equation (1).

normalized  $\Delta\epsilon'/\epsilon'(4K)$  and  $\left[\frac{M}{M(4K)}\right]^2$  as shown in Fig. 9 establishes a strong evidence for the presence of non-linear magneto-electric coupling in  $\alpha$ - $\text{Cu}_2\text{V}_2\text{O}_7$ .

The temperature variation of  $\epsilon'$  (Fig. 8(d)) in the low temperature region for the  $x = 0.3$  sample does not show any hump-like anomaly. This result is consistent with our structural characterization result where a Zn mediated phase transition from the  $\alpha$  to the  $\beta$  phase is noted beyond  $x_c = 0.15$ . So, it is evident that  $\text{Cu}_{2-x}\text{Zn}_x\text{V}_2\text{O}_7$  with  $x = 0.3$  is not expected to show any magneto-electric coupling due to its non-polar ( $\beta$  phase) structure as explained later.

The variation of the imaginary part of dielectric susceptibility ( $\epsilon''$ ), i.e., dielectric loss as a function of temperature for  $x = 0.0$  is shown in Fig. 10. At high temperature,  $\epsilon''$  increases with a rise in temperature, which may be due to space charge polarization. Although some anomaly is shown by  $\epsilon''(T)$  in the low temperature region between 10 K and 40 K (as shown in the inset of Fig. 10), the nature of this complex structure is not clear so far to draw any conclusion. Such behavior continues up to Zn concentration  $x = 0.15$ , but no such anomaly in  $\epsilon''$  is noticed for the  $x = 0.3$  sample.

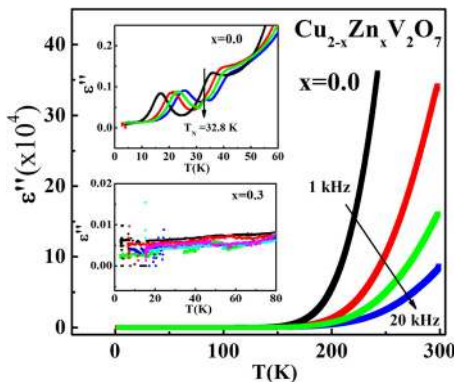


FIG. 10. Temperature dependence of the imaginary part of dielectric susceptibility ( $\epsilon''$ ) for the frequency range 1 kHz–20 kHz for the  $x = 0.0$  sample. Insets show a magnified low temperature part for  $x = 0.0$  and  $x = 0.3$ .

Our experimental result gives us a support to conclude that  $\alpha$ - $\text{Cu}_2\text{V}_2\text{O}_7$  is a magnetic ordering induced multiferroic material, while nonmagnetic Zn doping gradually suppresses its weak FM and ferroelectric properties below  $T_N$ . Our structural studies clearly show that Zn doping induces  $\alpha$ - to  $\beta$ -phase transition in this system, which is not unexpected since  $\beta$ - $\text{Cu}_2\text{V}_2\text{O}_7$  is iso-structural with  $\alpha$ - $\text{Zn}_2\text{V}_2\text{O}_7$ . The DM interaction is a microscopic characteristic of two interacting spins.<sup>19,20</sup> It favours canting of spins inducing a non-collinear spin ordering and weak FM moment. It occurs due to the existence of an asymmetric bonding geometry in an AF spin lattice background. In  $\alpha$ - $\text{Cu}_2\text{V}_2\text{O}_7$ , two mutually perpendicular Cu chains are present (Fig. 1), and each Cu atom is coupled to its nearest-neighbor (NN) by two asymmetric bonds or two exchange paths.<sup>17</sup> Due to these two asymmetric exchange paths, two DM vectors arise, which do not cancel each other, inducing a net DM interaction. On the other hand, the  $\beta$  phase in which NN Cu atoms are coupled by symmetric Cu-O-Cu bonds is forbidden by the DM interaction (Ref. 17 and references therein). The non-collinear spin ordering in the  $\alpha$ -phase is associated with a small shift of the ligand oxygen ions by which the system minimizes its energy, and as a result, a non-zero ferroelectric polarization appears. As discussed in Ref.17, Zn induced  $\alpha$ - to  $\beta$  phase transition may be due to the shortening of the apical M-O bond and the lengthening of the equatorial bonds of  $\text{MO}_5$  polyhedra (M = Cu and Zn). The elongation of the  $\text{CuO}_5$  polyhedra is expected since  $\text{Cu}^{2+}$  is a Jahn-Teller active ion. On the other hand, no distortion has been shown by  $\text{ZnO}_5$  polyhedra since  $\text{Zn}^{2+}$  is not Jahn-Teller active. As a result, the local bonding geometry will change with Zn substitution at the Cu site, and this explains the possible reason for the  $\alpha \rightarrow \beta$  phase transition of  $\alpha$ - $\text{Cu}_2\text{V}_2\text{O}_7$  through Zn doping. Hence, multiferroism is absent in  $\text{Cu}_{2-x}\text{Zn}_x\text{V}_2\text{O}_7$  when  $x > 0.15$ . In summary, our Zn doping studies may infer that ferroelectricity appears in  $\alpha$ - $\text{Cu}_2\text{V}_2\text{O}_7$  only due to the presence of the DM interaction, which favors canting of spins with an associated weak ferromagnetism but is completely absent in its  $\beta$  phase.

#### IV. CONCLUSION

The effect of non-magnetic Zn doping on the  $\alpha$ -phase of the  $\text{Cu}_2\text{V}_2\text{O}_7$  system has been studied, and we have observed a Zn mediated phase transition from the  $\alpha$ -phase to the  $\beta$ -phase beyond a critical Zn concentration  $x_c = 0.15$ .  $\alpha$ - $\text{Cu}_2\text{V}_2\text{O}_7$  maintains its canted AF structure with an associated weak FM due to the presence of the DM interaction up to Zn concentration  $x_c = 0.15$ , but beyond that, it becomes purely AF in the  $\beta$ -phase. The temperature dependence of the heat capacity data for the  $x_c = 0.15$  sample also confirms the presence of a clear anomaly corresponding to the temperature of anomaly in the magnetic susceptibility, indicating a clear evidence of a long range magnetic ordering. The presence of a non-linear magneto-electric coupling is revealed through dielectric studies only in the  $\alpha$ -phase of  $\text{Cu}_2\text{V}_2\text{O}_7$ .  $\alpha$ - $\text{Cu}_2\text{V}_2\text{O}_7$  presents itself as a promising magnetic multiferroic for future use.

- <sup>1</sup>O. Auciello, J. F. Scott, and R. Ramesh, *Phys. Today* **51**(7), 22 (1998).
- <sup>2</sup>A. Kumar, N. Ortega, S. Dussan, S. Kumari, D. Sanchez, J. Scott, and R. Katiyar, *Solid State Phenom.* **189**, 1 (2012).
- <sup>3</sup>C. W. Nan, M. I. Bichurin, S. Dong, D. Viehland, and G. Srinivasan, *J. Appl. Phys.* **103**, 031101 (2008).
- <sup>4</sup>D. Khomskii, *Physics* **2**, 20 (2009).
- <sup>5</sup>N. A. Spaldin, S. W. Cheong, and R. Ramesh, *Phys. Today* **63**(10), 38–43 (2010).
- <sup>6</sup>D. I. Khomskii, *J. Magn. Magn. Mater.* **306**, 1 (2006).
- <sup>7</sup>A. Kumarasiri, E. Abdelhamid, A. Dixit, and G. Lawes, *Phys. Rev. B* **91**, 014420 (2015).
- <sup>8</sup>T. Kimura, T. Goto, H. Shintani, K. Ishizaka, T. Arima, and Y. Tokura, *Nature* **426**, 55 (2003).
- <sup>9</sup>N. Hur, N. S. Park, P. A. Sharma, J. S. Ahn, S. Guha, and S.-W. Cheong, *Nature* **429**, 392 (2004).
- <sup>10</sup>C. Calvo and R. Faggiani, *Acta Crystallogr., B* **31**, 603 (1975).
- <sup>11</sup>M. Touaiher, K. Rissouli, K. Benkhouja, M. Taibi, J. Aride, A. Boukhari, and B. Heulin, *Mater. Chem. Phys.* **85**, 41 (2004).
- <sup>12</sup>J. Sannigrahi, S. Bhowal, S. Giri, S. Majumdar, and I. Dasgupta, *Phys. Rev. B* **91**, 220407(R) (2015).
- <sup>13</sup>G. Gitgeatpong, Y. Zhao, M. Avdeev, R. O. Piltz, T. J. Sata, and K. Matan, *Phys. Rev. B* **92**, 024423 (2015).
- <sup>14</sup>A. A. Tsirlin, O. Janson, and H. Rosner, *Phys. Rev. B* **82**, 144416 (2010).
- <sup>15</sup>M. Sánchez-Andújar, S. Yáñez-Vilar, J. Mira, N. Biskup, J. Rivas, S. Castro-García, and M. A. Señaris-Rodríguez, *J. Appl. Phys.* **109**, 054106 (2011).
- <sup>16</sup>L. A. Ponomarenko, A. N. Vasil'ev, E. V. Antipov, and Yu. A. Velikodny, *Physica B* **284–288**, 1459 (2000).
- <sup>17</sup>J. Pommer, V. Kataev, K.-Y. Choi, P. Lemmens, A. Ionescu, Yu. Pashkevich, A. Freimuth, and G. Güntherodt, *Phys. Rev. B* **67**, 214410 (2003).
- <sup>18</sup>K. Sotojima, R. O. Suzuki, K. Amezawa, and Y. Tomii, *Mater. Trans.* **48**(8), 2094 (2007).
- <sup>19</sup>I. Dzyaloshinsky, *Phys. Chem. Solids* **4**, 241 (1958).
- <sup>20</sup>T. Moriya, *Phys. Rev.* **120**, 91 (1960).
- <sup>21</sup>Y.-W. Lee, T.-H. Jang, S. E. Dissanayake, S. Lee, and Y. H. Jeong, *EPL* **113**, 27007 (2016).
- <sup>22</sup>V. Kataeva, J. Pommer, K.-Y. Choi, P. Lemmens, A. Ionescu, Y. Pashkevich, K. Lamonova, A. Moller, A. Freimuth, and G. Guntherodt, *J. Magn. Magn. Mater.* **272–276**, 933 (2004).
- <sup>23</sup>A. Dixit and G. Lawes, *J. Phys.: Condens. Matter* **21**, 456003 (2009).
- <sup>24</sup>Z. He, J.-I. Yamaura, and Y. Ueda, *J. Solid State Chem.* **181**, 2346 (2008).
- <sup>25</sup>S. Bhattacharjee, V. Pandey, R. K. Kotnala, and D. Pandey, *Appl. Phys. Lett.* **94**, 012906 (2009).
- <sup>26</sup>D. L. Fox, D. R. Tilley, J. F. Scott, and H. J. Guggenheim, *Phys. Rev. B* **21**, 2926 (1980).